Contents lists available at ScienceDirect

Toxicology

journal homepage: www.elsevier.com/locate/toxicol

Effect of heated tobacco products and traditional cigarettes on pulmonary toxicity and SARS-CoV-2-induced lung injury

Han-Hsing Tsou [a,b,1], Ping-Huai Wang [c,d,1], Tzu-Hsin Ting [a], Yueh-Hsin Ping [e,f], Tsung-Yun Liu [a,g], Hsiao-Wei Cheng [e], Hsiang-Tsui Wang [a,e,h,*]

[a] *Institute of Food Safety and Health Risk Assessment, National Yang Ming Chiao Tung University, Taipei, Taiwan*
[b] *Kim Forest Enterprise Co., Ltd., Taipei 112, Taiwan*
[c] *Division of Pulmonology, Department of Internal Medicine, Far Eastern Memorial Hospital, New Taipei City 220, Taiwan*
[d] *Department of Nursing, Oriental Institute of Technology, New Taipei City, Taiwan*
[e] *Institute of Pharmacology, College of Medicine, National Yang Ming Chiao Tung University, Taipei, Taiwan*
[f] *Institute of Biophotonics, National Yang Ming Chiao Tung University, Taipei, Taiwan*
[g] *Institute of Environmental and Occupational Health Sciences, National Yang Ming Chiao Tung University, Taipei, Taiwan*
[h] *Doctor Degree Program in Toxicology, Kaohsiung Medical University, Kaohsiung, Taiwan*

ARTICLE INFO

ABSTRACT

Cigarette smoke (CS) significantly contributes to the development of chronic obstructive pulmonary disease (COPD). Heated tobacco products (HTPs), newly developed cigarette products, have been proposed as an alternative for safe cigarette smoking. Although it is plausible to think that replacing traditional cigarettes with HTPs would lower the risks of COPD, this notion requires confirmation by further investigations from sources independent of the tobacco industry. COPD is characterized by an ongoing inflammatory process in the lungs, and the renin-angiotensin system (RAS) has been implicated in the pathogenesis of COPD. Angiotensin-converting enzyme-2 (ACE2) functions as a negative regulator of RAS and has been suggested as a cellular receptor for the causative agent of SARS-CoV-2. It has been shown that smoking is most likely associated with the negative progression and adverse outcomes of SARS-CoV-2. In this study, we found that cigarette smoke extracts from traditional cigarettes (CSE) caused higher cytotoxicity and higher oxidative stress levels than extracts from HTPs (HTPE) in two lung cell lines (Calu-3 and Beas-2B). CSE and HTPE induced RAS activation, MAPK activation, and NF-kB inflammatory pathway activation, resulting in the production of inflammatory cytokines. Furthermore, CSE and a high dose of HTPE reduced tight junction proteins, including claudin 1, E-cadherin, and ZO-1, and disrupted lung epidermal tight junctions at the air-liquid interface (ALI). Finally, CSE and HTPE enhanced the spike protein S1-induced lung injury response. Together, these results suggest that HTPE induced similar lung pathogenesis relevant to COPD and SARS-CoV-2-induced lung injury caused by CSE.

1. Introduction

Cigarette smoke (CS) contains over 7000 chemicals, many of which are products of incomplete combustion and the thermogenic degradation of tobacco cigarettes (Soleimani et al. 2022). Epidemiological studies have reported that inhalation exposure to CS causes pulmonary toxicity and the onset of chronic obstructive pulmonary disease (COPD), chronic bronchitis, and asthma (Esposito et al. 2014; Hoek et al. 2013). These health risks have led to the development of materials that may assist people in quitting smoking, including heated tobacco products

(HTPs). Manufacturers' allegations that HTPs are "safe" are questionable, and studies on the adversity of HTP vapors to respiratory airways have yielded conflicting results (Biondi-Zoccai et al. 2019; Paumgartten, 2018; Simonavicius et al. 2018; Tabuchi et al. 2016). HTPs are electronic devices that heat-process tobacco instead of combusting it to supposedly deliver an aerosol with fewer toxicants than traditional cigarettes (Glantz 2018a). However, current studies on HTP emissions and human use vary by methodology, products, and comparators, and these studies are primarily affiliated with manufacturers (Simonavicius et al. 2018). Thus, further investigations require confirmation, including inhalation toxicological studies, and this information should come from sources independent of the tobacco industry.

COPD is characterized by an ongoing inflammatory process in the lungs that drives airway and lung tissue remodeling, including airway fibrosis and emphysematous lung tissue destruction (Barnes et al. 2015). The initial activation induces the production of proinflammatory cytokines, such as interleukin 1-beta (IL-1β), interleukin 6 (IL-6), interleukin 8 (IL-8), and tumor necrosis factor-alpha (TNFα), leading to further propagation of the inflammatory response (Lee and Downey, 2001). The prolonged and uncontrolled release of these cytokines alters different intercellular signaling pathways, leading to barrier dysfunction (Aghapour et al. 2018). Bronchial epithelial barrier function, as a frontline defense, is maintained by apical junctional complexes that form between neighboring cells and consist of apical tight junctions (TJs) underlying adherens junctions (AJs) (Tsukita et al. 2019). TJ proteins, such as the claudin family, zonula occludens (ZO) proteins, and AJ proteins, such as E-cadherin, compose the junctional complexes in the bronchial epithelium (Rezaee and Georas, 2014). In recent studies, weaker expression levels of ZO-1, occludin, and E-cadherin were observed in bronchial epithelium and lung tissue sections from COPD patients than in healthy individuals, suggesting a broad defect in adhesion mechanisms in COPD (Aghapour et al. 2018; Heijink et al. 2014; Nishida et al. 2017). In response to cigarette smoke, acute changes in epithelial permeability and decreases in several essential TJ and AJ proteins have been noted (Heijink et al. 2012; Oldenburger et al. 2014; Schamberger et al. 2014).

The renin-angiotensin system (RAS) has been implicated in the pathogenesis of COPD through the stimulation of proinflammatory mediators in the lung (Kaparianos and Argyropoulou, 2011; Kuba et al. 2006; Marshall, 2003; Shrikrishna et al. 2012). RAS can also generate reactive oxygen species (ROS), thereby promoting mitochondrial dysfunction and contributing to the oxidative stress and endothelial dysfunction observed in patients with COPD (Benigni et al. 2010; Rahman and Adcock, 2006). Angiotensin-converting enzyme-2 (ACE2) functions as a negative regulator of RAS and has been suggested as a cellular receptor for the causative agent of SARS-CoV-2 (Zhang et al. 2020a). ACE2 has well-established anti-inflammatory and antioxidant properties through the reduction in angiotensin II (Ang II) and the elevation of angiotensin-(1−7) (Ang-(1−7)) (Donoghue et al. 2000; Tipnis et al. 2000). Therefore, the benefits of ACE2 on the lungs have been suggested to protect against acute lung injury in several animal models of acute respiratory distress syndrome (ARDS) (Jerng et al. 2006; Marshall et al. 2002; Raiden et al. 2002). Thus, the RAS appears to play a critical role in the pathogenesis of acute lung injury.

Current scientific literature has shown some controversial results between smoking and susceptibility to SARS-CoV-2 infection (Liu et al. 2020; Vardavas and Nikitara, 2020). The susceptibility to SARS-CoV-2 infection and the chance of adverse health outcomes with SARS-CoV-2 infection in the general population are variable (Chen et al. 2020; Guan et al. 2020a). It has been shown that smoking is most likely associated with the negative progression and adverse consequences of SARS-CoV-2 (Guan et al. 2020b; Zhang et al. 2020b); however, the underlying mechanisms remain elusive. Therefore, the effects of smoking, including traditional CS and HTPs, on RAS and how these effects are involved in the pathogenesis of COPD were investigated in bronchial epithelium cultured in a conventional 2D dish and at the 3D air-liquid interface (ALI). Furthermore, the effects of traditional CS and HTPs on

SARS-CoV-2-induced lung injury responses were also examined.

2. Materials and methods

2.1. Preparation of HTP and CS extracts

The preparation of the tar phase extract of aerosol induced by HTP heat-sticks (Philip Morris, Tokyo, Japan) (1.4 mg nicotine) or L&M green label cigarettes (Philip Morris, Washington, DC, USA) (1.2 mg nicotine) by puff smoking conditions is described in the Supplementary Materials.

2.2. Nicotine analysis

Nicotine levels were analyzed in CSE or HTPE using the Acquity UPLC/TQD system (Waters, Milford, MA) as described in the Supplementary Materials.

2.3. Cell culture

Human lung adenocarcinoma (Calu-3) and human bronchial epithelium (Beas-2B) cells were purchased from ATCC and maintained in Dulbecco's modified Eagle's medium (DMEM) supplemented with 10% FBS and RPMI 1640 medium supplemented with 10% FBS, respectively.

2.4. Three-dimensional organotypic lung epithelium air-liquid interface (ALI) model

The development of a standardized three-dimensional (3D) system of human bronchial epithelial cells based on Calu-3 cells was performed (Stewart et al. 2012) as described in the Supplementary Materials.

2.5. Treatment with HTP and CS extracts

For a conventional 2D culture, cells were seeded for 24 h and then treated with CSE or HTPE (0–0.5 mg/mL) for 24 h. For the 3D ALI culture system, on Day 10 of ALI culture, cells were washed with PBS buffer, and CSE or HTPE (400 μl) was added to the basolateral side of the ALI cultures and incubated for 24 h at 37 °C in the dark.

2.6. Treatment with spike protein S1

We treated Calu-3 cells with SARS-CoV-2 spike protein S1 (aa 14–683) (Invitrogen # RP-87681, 10 ng/mL) for 0, 4, and 24 h after treatment with CSE or HTPE for 24 h. Since spike protein S1 was fused to His-Avi Tag at the C-terminus, cells were stimulated with the peptide encoding the His-Avi Tag (His-Avi as a negative control).

2.7. Cytotoxicity assay

Cytotoxicity was determined using a modified 3-(4,5- dimethylthiazol-2-yl)− 2,5-diphenyl tetrazolium (MTT; Sigma, St. Louis, MO) assay and a lactate dehydrogenase (LDH) leakage assay as described previously (Mosmann, 1983).

2.8. Dichlorofluorescein (DCF) assay (Intracellular ROS)

After exposure, the cells were washed with PBS (Gibco, 10270) and then incubated at 37 °C in 5% CO2 with 10 μM of a 5- (and-6)-chloromethyl-2′,7′-dichlorodihydrofluorescein diacetate (CM-H2DCFDA) probe (Sigma) in PBS (0.5 mL/well or insert) for 35 min. After 30 min of incubation, the probe was removed from the wells, and the cells were harvested. Levels of pro-oxidants were determined by flow cytometry (FACSCalibur, BD).

2.9. Determination of phosphatidylserine (PS) externalization by Annexin V-FITC staining

Cells (1×10^6/10-cm dish) were analyzed by FITC Annexin V (Bio-Legend, USA) according to the manufacturers' instructions. Briefly, cells were stained with 5 μl of FITC Annexin V and 10 μl of PI (0.5 mg/mL) for 15 min at room temperature in the dark, followed by flow cytometry analysis with a Becton-Dickinson FACScan instrument and Cell Quest software.

2.10. Quantification of angiotensin II and inflammatory cytokines by ELISA

Levels of angiotensin II and inflammatory cytokines were measured in culture media collected after 24 h of exposure and kept at − 80 °C until analysis. Before freezing, the culture media were centrifuged for 5 min at 3600 rpm at 4 °C to remove the cells. Angiotensin II, IL-6, Il-1β, and TNF-α release were measured using a commercially available Angiotensin II EIA Kit (Sigma, RAB0010), an IL-6 Human ELISA kit (Invitrogen, EH2IL6), an IL-1β Human ELISA kit (Invitrogen, BMS224–2) and a TNF alpha Human ELISA kit (Invitrogen, BMS223HS), respectively, according to the manufacturer's instructions.

2.11. Transepithelial electrical resistance (TEER) assay

Tissue integrity after exposure was determined on three inserts per treatment. Cellular TEER was measured using a Millicell ERS-2 Epithelial Voltohmmeter (Merck KGaA, Darmstadt, Germany) after adding 200 μl medium to the apical side of the cells.

2.12. Permeability assay

One hundred microliters of medium containing fluorescein isothiocyanate (FITC)-dextran (4 kDa, Sigma—Aldrich) (1 mg/mL) and 500 μl of medium were added to the apical and basal chambers, respectively. Then, the cells were incubated for 30, 60 and 180 min, and the culture medium in the basal chamber was collected to measure fluorescence using an ELISA reader (TECAN Sunrise). The excitation and emission wavelengths were 488 and 525 nm, respectively.

2.13. Quantitative real-time RT—PCR

The procedure and the sequences of all the primers are shown in the Supplementary Materials.

2.14. Immunoblotting analysis

Cells were exposed to CSE or HTPE for 24 h, rinsed, and immediately placed in RIPA buffer. Cell lysates were prepared and analyzed as described previously (Wang et al. 2012). Briefly, blots were probed with primary antibodies as shown in the Supplementary Materials. The immunoreaction was visualized using enhanced chemiluminescence (ECL) (Millipore Corporation, Billerica, MA).

2.15. Histological examination and immunofluorescence staining

After cultures were grown for 10 days under ALI conditions and 24 h postexposure to CSE or HTPE, the membranes were removed from the transwells, cultures were fixed with 10% buffered formalin (Sigma), and samples were embedded in wax, cut into transverse sections, and stained with hematoxylin and eosin (H&E). Immunofluorescent staining was conducted for tight junction proteins as previously described (Wang et al. 2016). The following antibodies were used at the noted dilutions: anti-claudin-1 (1:100, GenTex, GTX134842), anti-E-cadherin (1:100, Cell Signaling, #3195) or ZO-1 (1:100, Invitrogen, #40–2200) at 4 °C overnight. The cells were then washed, incubated in the appropriate

secondary antibody (Invitrogen, USA) for one hour at room temperature, incubated in DAPI (Sigma) to stain the nuclei, and mounted with coverslips. The stained slides were imaged using an Olympus FV1000 confocal laser microscope (Olympus, Japan).

2.16. Statistical analyses

Descriptive statistics are presented as the mean ± standard deviation or the number (percentage). Student's *t* tests were used to determine statistical significance. All calculated *p* values were two-tailed. Statistical significance was defined as $p < 0.05$. All analyses were performed with the IBM SPSS Statistics software package, version 23.0.

3. Results

3.1. Comparison of the cytotoxicity of cigarette smoke extracts from traditional cigarettes (CSE) or HTPs (HTPE) in human bronchial epithelium, Calu-3, and Beas-2B

Total particulate matter (TPM) was collected and extracted from L&M green label cigarettes and HTPs, namely, cigarette smoke extracts (CSE) and HTP extracts (HTPE), respectively (Supplementary Fig. 1). The nicotine levels in HTPE (0.1 mg/mL) and CSE (0.1 mg/mL) were 2.02 μM and 0.90 μM, respectively (Supplementary Fig. 2). The cytotoxicity of CSE and HTPE in human lung epithelial cells, including Calu-3 and Beas-2B cells, was analyzed using MTT. The results showed that CSE had higher cytotoxicity in Calu-3 and Beas-2B cells than HTPE. The IC_{50} values of CSE were 0.26 ± 0.21 mg/mL and 0.24 ± 0.40 mg/mL in Calu-3 and Beas-2B cells, respectively, while the IC_{50} of HTPE was higher than 1 mg/mL in both cell lines (Fig. 1**A**). A similar phenomenon was observed using the LDH assay (Fig. 1**B**). Furthermore, using Annexin V/PI assays, the results showed that CSE induced apoptosis in a dose-dependent manner and that 0.5 mg/mL HTPE slightly induced apoptosis in Calu-3 (Figs. 1**C,** 1**E**) and Beas-2B cells (Figs. 1**D,** 1**F**). Consistently, CSE induced higher levels of apoptosis markers, including the cleavage of caspase 9, caspase 3 and PARP, than HTPE in both Calu-3 and Beas-2B cells, as shown by Western blot analysis (Fig. 1**G-H**).

3.2. Regulation of the RAS, oxidative stress, and NF-kB inflammatory pathways was analyzed in Calu-3 and Beas-2B cells treated with CSE or HTPE

Previous studies have shown that the RAS is potentially implicated in the pathogenesis of COPD through its involvement in inducing proinflammatory mediators and oxidative stress in the lung (Marshall, 2003; Rahman and Adcock, 2006). Our results showed that the reduction in ACE2 expression and the increased the ratio of ACE1 to ACE2 mRNA expression significantly upregulated angiotensin II (Ang II) secretion in Calu-3 cells treated with CSE or HTPE (**upper panel of** Fig. 2**A,** Fig. 2**B,** Supplementary Fig. 3**A**). These results indicate that CSE or HTPE activated RAS. Furthermore, CSE activated downstream MAPK signaling pathways, including ERK and JNK, in Calu-3 cells; however, HTPE only activated the ERK pathway (Fig. 2**B**). Although a lack of ACE2 expression was observed in Beas-2B cells (Supplementary Fig. 3B), the secretion of Ang II expression was significantly upregulated (**lower panel of** Fig. 2**A**). Downstream ERK and JNK signaling was activated in Beas-2B cells treated with CSE or HTPE (Fig. 2**C**). The RAS can generate ROS, which contributes to the oxidative stress and impaired redox signaling observed in COPD (Rahman and Adcock, 2006). Our results showed that CSE, but not HTPE, induced the production of intracellular ROS in Calu-3 and Beas-2B cells using DCF assays (Fig. 2**D**). The redox-sensitive transcription factor nuclear factor (NF)-kappaB (NF-κB) is an essential participant in a broad spectrum of inflammatory networks that regulate cytokine activity in airway pathology (Edwards et al. 2009; Schuliga, 2015). We further analyzed NF-kB pathways and the production of inflammatory cytokines in Calu-3 and Beas-2B cells treated with CSE or
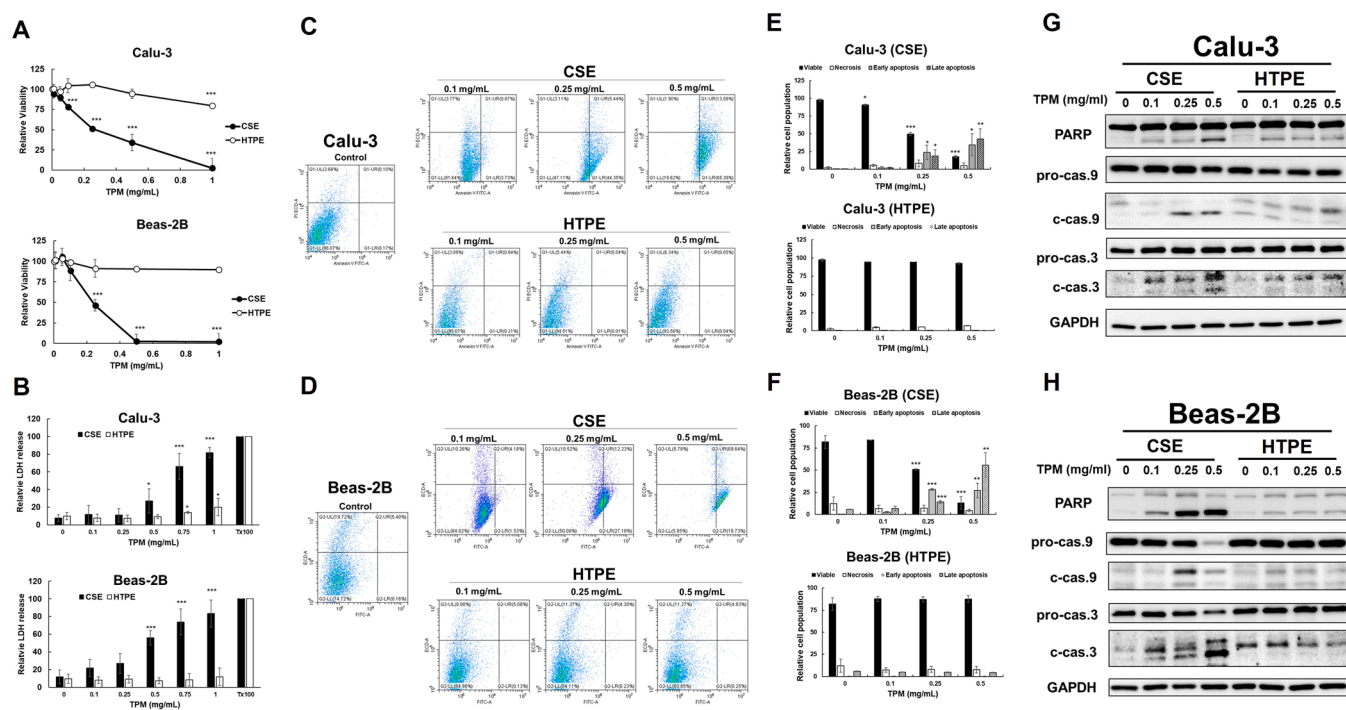
Fig. 1. Cytotoxicity and apoptosis pathway in Calu-3 cells or Beas-2B cells treated with CSE or HTPE. Cytotoxicity in Calu-3 cells Beas-2B cells was analyzed using (A) MTT or (B) LDH assays after 24 h treatment with CSE (0–1 mg/mL, upper panel) or HTPE (0–1 mg/mL, lower panel). (C-F) Flow cytometric analyses with annexin-V-FITC and PI staining in Calu-3 or Beas-2B treated with CSE (0–1 mg/mL) or HTPE (0–1 mg/mL) for 24 h. (C-D) Apoptosis is determined by staining with annexin-V+PI. Q1: necrotic, AV − /PI + ; Q2: late apoptotic, AV + /PI + ; Q3: live, AV − /PI − ; Q4: early apoptotic, AV + /PI − . (E-F) The percentage of cells in each group in Calu-3 (E) or Beas-2B (F). Values are presented as mean ± SD. Student's *t*-tests were used to determine statistical significance, and two-tailed p-values were shown. *p < 0.05, ***p < 0.005 compared with control group. (G-H) Western blot analysis of apoptotic pathway in (G) Calu-3 or (H) Beas-2B treated with CSE (0–0.5 mg/mL) or HTPE (0–0.5 mg/mL) for 24 h. pro-cas. 3/9: proform of caspase 3/9; c-cas. 3/9: cleavage form of caspase 3/9. A minimum of three independent experiments were performed.

HTPE. CSE or HTPE increased phosphorylated NF-kB and decreased IkB, indicating that CSE or HTPE induced the activation of NF-kB inflammatory pathways in Calu-3 and Beas-2B cells (Fig. 2**B-C**). The mRNA expression levels of downstream inflammatory cytokines, including IL-6, IL-1β, and TNF-α, were also upregulated in both cell lines (Supplementary Fig. 4). Consistently, the secretion levels of IL-6, IL-1β, or TNFα were upregulated in culture medium collected from Calu-3 and Beas-2B cells treated with CSE or HTPE (Fig. 2**E-J**). Notably, HTPE induced higher IL-1β secretion in both cell lines than CSE on an equal concentration basis (Figs. 2**F**, 2**I**). These results indicate that alteration of the RAS system, activation of the downstream MAPK and NF-kB pathways, and upregulation of downstream inflammatory gene expression were observed in Calu-3 and Beas-2B cells treated with CSE or HTPE.

3.3. The expression of tight junction proteins was analyzed in Calu-3 and Beas-2B cells treated with CSE or HTPE

Previous studies have shown that prolonged and uncontrolled inflammatory cytokine release leads to epithelial barrier dysfunction (Aghapour et al. 2018). We further investigated the effect of CSE or HTPE on the expression of tight junction proteins in Calu-3 and Beas-2B cells. In both cell lines, CSE or HTPE downregulated tight junction protein expression, including claudin 1, ZO-1, and E-cadherin (Fig. 3**A-B**). Immunofluorescence staining for claudin-1, E-cadherin, and ZO-1 revealed a well-defined localization around cell borders in Calu-3 cells treated with vehicle control, indicating the presence of intact tight junctions (Fig. 3**C**). Meanwhile, the staining of these tight junction proteins was not limited to cellular boundaries in Calu-3 cells after CSE or HTPE exposure for 24 h (Fig. 3**C**), indicating disruption of tight junctions. Although we did not observe intact tight junctions in Beas-2B

cells, we found that CSE or HTPE decreased the expression of tight junction proteins (Fig. 3**D**), which is similar to the above results (Fig. 3**B**).

Furthermore, Calu-3 cells were cultured in ALI, and epithelial barrier function was evaluated by TEER measurements and permeability assays (Fig. 4**A-E**). The results showed that CSE (0.1–0.5 mg/mL) or a high dose of HTPE (0.5 mg/mL) significantly reduced TEER after 6 h of treatment, although the level of TEER reduction induced by HTPE was not the same as that induced by CSE (Fig. 4**B-C**). Additionally, 24 h treatment with CSE (0.1–0.5 mg/mL) or a high dose of HTPE (0.5 mg/mL) significantly reduced TEER (Fig. 4**D**) and increased fluorescence signals after the addition of FITC-conjugated dextran (4 kDa, Sigma) at 30, 90 or 120 min (Fig. 4**E**). These results suggest that CSE or a high dose of HTPE increased lung epithelial permeability. Consistently, CSE and a high dose of HTPE downregulated the expression of tight junction proteins, including claudin 1, ZO-1, and E-cadherin, in Calu-3 cells in ALI (Fig. 4**F**). Furthermore, histological examination of Calu-3 cells in ALI showed that CSE or HTPE (0.5 mg/mL) led to the development of epithelial remodeling with the appearance of a disordered epithelium compared to unexposed cells (Fig. 4**G**). Upon further evaluation of the cytotoxicity of CSE or HTPE in Calu-3 cells cultured in ALI using the LDH assay, the results showed that the doses (0.1, 0.25, 0.5 mg/mL) used for CSE or HTPE did not induce significant cytotoxicity (Supplementary Fig. 5). Furthermore, we found that CSE or HTPE activated NF-kB pathways (Supplementary Fig. 6**A**), and the secretion levels of IL-6, IL-1β, and TNF-α were also upregulated by Calu-3 in ALI (Supplementary Fig. 6**B**-**D**). Together, these results indicate that both CSE and HTPE disrupt tight junctions and induce the release of inflammatory cytokines in Calu-3 cells in ALI.
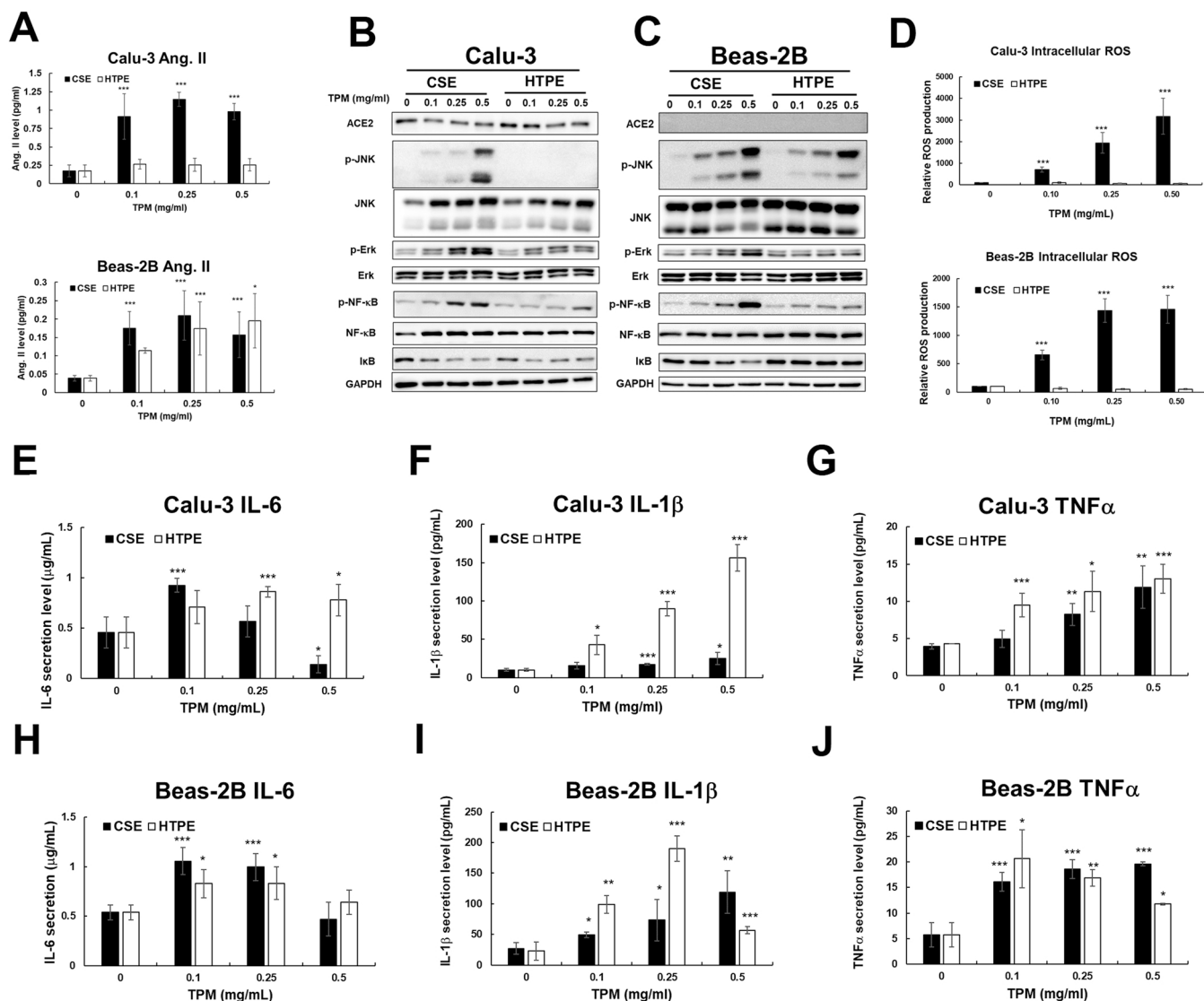
Fig. 2. The effect of CSE and HTPE on RAS, the production of ROS, and NF-kB inflammatory pathways in Calu-3 and Beas-2B cells. Calu-3 or Beas-2B were treated with CSE (0–0.5 mg/mL) or HTPE (0–0.5 mg/mL) for 24 h. (A) The secretion of angiotensin II (Ang. II) in Calu-3 (upper panel) or Beas-2B (lower panel) was analyzed using the Angiotensin II ELISA kit (Sigma). (B-C) Western blot analysis of ACE2 and downstream MAPK pathway including p-JNK, JNK, p-Erk, and Erk, and NF-kB inflammatory pathways including p-NF-kB, NF-kB, and IkB in (B) Calu-3 or (C) Beas-2B. (D) the production of intracellular ROS in Calu-3 (upper panel) or Beas-2B (lower panel) using DCF assays. (E-J) The secretion of IL-6, IL-1β, and TNFα in (E-G) Calu-3 or (H-J) Beas-2B cells was analyzed using IL-6, IL-1β, and TNFα ELISA kit (Invitrogen). Values are presented as mean ± SD. Student's *t*-tests were used to determine statistical significance, and two-tailed p-values were shown. $*p < 0.05$, $**p < 0.01$, $***p < 0.005$ compared with control group. A minimum of three independent experiments were performed.

3.4. The impact of CSE and HTPE on SARS-CoV-2 spike protein-induced lung injury responses

ACE2 has been suggested as a cellular receptor for SARS-CoV-2 (Zhang et al. 2020a), and high ACE2 expression in Calu-3 cells but not in Beas-2B cells was observed (Supplementary Fig. 3B). Therefore, we used Calu-3 cells as a model to analyze lung injury responses induced by the SARS-CoV-2 spike protein S1. SARS-CoV-2 utilizes spike proteins to bind to the host cell receptor ACE2, mediating viral cell entry (Letko et al. 2020). To mimic the binding process of SARS-CoV-2 infection and study SARS-CoV-2-induced cellular injury, we stimulated Calu-3 cells with the SARS-CoV-2 spike protein S1 (aa 14–683) in the presence of CSE or HTPE. The results showed that the ratio of ACE1 to ACE2 was upregulated in Calu-3 cells treated with spike protein S1 for 4 h or 24 h (Supplementary Fig. 7A). Furthermore, spike protein S1 induced the secretion of Ang II in Calu-3 cells after treatment for 4 h or 24 h (Fig. 5A). Consequently, downstream signaling pathways, including the

MAPK and NF-kB inflammatory pathways, were activated after treatment with spike protein S1 (Fig. 5B). The mRNA expression levels of the downstream inflammatory cytokines IL-6, IL-1β, and TNF-α were also upregulated in both cell lines (Supplementary Fig. 7B–D). Consistently, the secretion levels of IL-6, IL-1β, and TNFα were upregulated in culture medium collected from Calu-3 and Beas-2B cells treated with CSE or HTPE (Fig. 5C-E). More importantly, our results demonstrated that CSE or HTPE (0.5 mg/mL) enhanced the reduction of ACE2, the activation of RAS, downstream MAPK pathways, and NF-kB pathways, and ultimately enhanced the release of inflammatory cytokines, which was attributed to spike protein S1 (Fig. 5, Supplementary Fig. 7).

4. Discussion

Current studies on the adversity of HTP vapors to respiratory airways have yielded conflicting results (Biondi-Zoccai et al. 2019; Dinakar and O'Connor, 2016; Paumgartten, 2018; Polosa and Caponnetto, 2016;
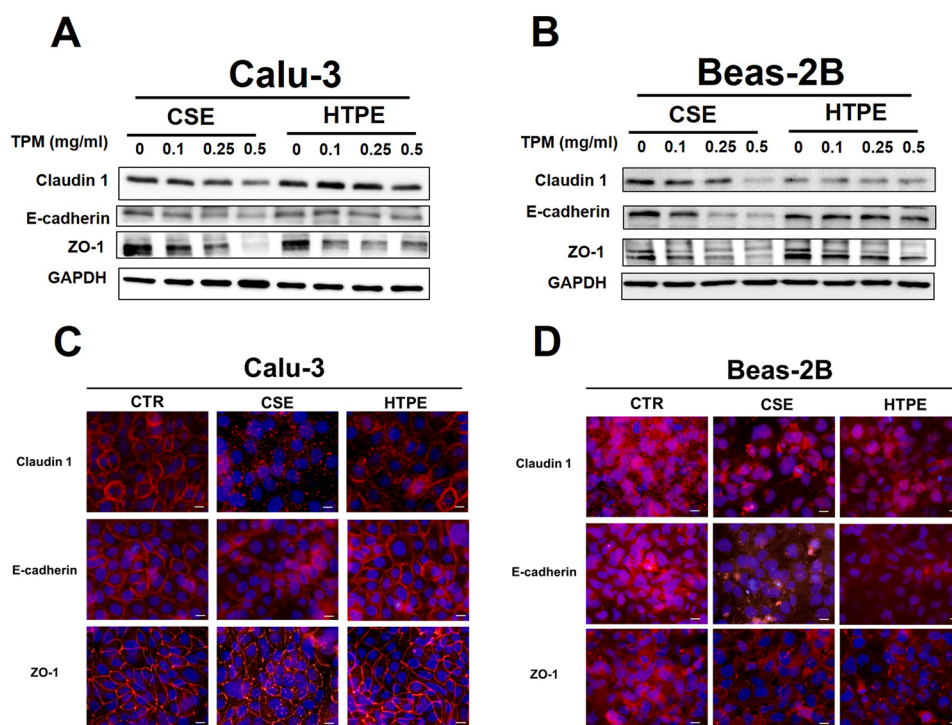
Fig. 3. The effect of CSE and HTPE on the expression of tight junction proteins and epithelial barrier function. Calu-3 or Beas-2B were treated with CSE (0–0.5 mg/mL) or HTPE (0–0.5 mg/mL) for 24 h. (A-B) Western blot analysis of tight junction proteins including claudin-1, E-cadherin, and ZO-1 in (A) Calu-3 or (B) Beas-2B (C&D) Immunofluorescent staining assay for tight junction proteins including claudin-1, E-cadherin, ZO-1 in (C) Calu-3 or (D) Beas-2B treated with CSE (0.25 mg/mL) or HTPE (0.25 mg/mL) for 24 h. Scale bar = 50 μm. A minimum of three independent experiments were performed.

Simonavicius et al. 2018; Tabuchi et al. 2016). Despite claims of reduced harmful effects by the tobacco industry, the adverse health effects of HTPs on lung pathogenesis relevant to COPD and the SARS-CoV-2-induced lung injury response remain elusive. Our study indicates that HTPE, similar to CSE, induced lung pathogenesis pertinent to COPD, including the alteration of the RAS system, increased inflammation, and disruption of lung epidermal tight junctions. Furthermore, HTPE also enhanced the spike protein S1-induced lung injury response comparable to CSE. These results indicate that HTPE can potentially induce chronic lung diseases, i.e., COPD, and enhance the SARS-CoV-2-induced lung injury response. To the best of our knowledge, this is the first report to show the effect of acute HTPE exposure on the SARS-CoV-2-induced lung injury response.

This study found that CSE caused higher cytotoxicity and higher ROS production than HTPE in Calu-3 and Beas-2B cells using MTT and LDH assays (Fig. 1A-B, Fig. 2D). The results are similar to those of previous studies showing that TPM collected from HTPs induced lower cytotoxicity using lung epithelial cells (Davis et al. 2019; Ito et al. 2020). Furthermore, recent studies reported that the gas vapor phase, TPM, or whole aerosol/smoke collected from HTPs does not decrease cell viability in various types of respiratory cells through leakage of the plasma membrane by the LDH assay (Davis et al. 2019). However, they affect critical cell functions such as metabolic activity via mitochondrial reductase function, as seen with the MTT assay (Davis et al. 2019; Leigh et al. 2018). While it has been reported that HTPs generated lower levels of ROS than combustible cigarettes in human lung fibroblast cells (Lyu et al. 2022) or Jurkat T cells (Scharf et al. 2021), HTPs have also been shown to have similar potential as conventional cigarette products to induce an oxidative stress response in rat alveolar epithelial cells (Ito et al. 2020). These results indicate that the cytotoxicity or oxidative stress induced by conventional cigarettes and HTPs was affected by cell types, endpoint assays, and various components of smoke/aerosols.

RAS has been implicated in the pathogenesis of COPD through activation of downstream MAPK and NF-kB pathways and stimulation of proinflammatory mediators in the lung (Kaparianos and Argyropoulou, 2011; Kuba et al. 2006; Marshall, 2003; Shrikrishna et al. 2012). We found that CSE had a higher detrimental effect on the production of Ang

II and activation of MAPK than HTPE in the 2D culture of Calu-3 cells (**upper panel of** Figs. 2A, 2B). However, the above effects were similar in Beas-2B cells treated with CSE and HTPE (**lower panel of** Figs. 2A, 2C). In both Calu-3 and Beas-2B cells, our results demonstrated that CSE or HTPE induced the secretion of IL-6, IL-1β, or TNFα (Fig. 2E-J); interestingly, HTPE induced higher IL-1β secretion than CSE on an equal concentration basis (Figs. 2F, 2I). Various studies have shown that HTPs induce fewer proinflammatory cytokines, including IL-6, IL-1β, IL-8 and TNFα, in different lung cell lines than conventional cigarettes (Dusautoir et al. 2021; Ito et al. 2020; Leigh et al. 2018; Lyu et al. 2022; Munakata et al. 2018; Scharf et al. 2021). There are three factors that could account for these variations in results: first, different cell culture systems, including submerged and ALI cell culture, were used; second, different protocols of cell exposure, such as exposure to aerosol extracts or direct aerosol exposure, were employed and could lead to different compositions of conventional cigarettes or HTPs; third, different cell types, which can express different levels of oxidative capacity, metabolic activity, and sensitivity to exogenous materials, were evaluated (Lujan et al. 2019). Beas-2B cells are derived from the normal bronchial epithelium, and Calu-3 cells are derived from the pleural effusion of a patient with adenocarcinoma of the lung; thus, cell characteristics cause different responses toward CSE and HTPE. In addition, high ACE2 expression was observed in Calu-3 cells but not in Beas-2B cells (Supplementary Fig. 3B). Both CSE and HTPE enhanced the spike protein S1-induced lung injury response, including RAS activation, downstream MAPK pathways, and NF-kB pathways, and enhanced the expression of inflammatory cytokines in Calu-3 cells (Fig. 5). However, this phenomenon was not observed in Beas-2B cells (Supplementary Fig. 8).

Our results showed that CSE or HTPE induced a reduction in ACE2 protein expression in Calu-3 cells, leading to RAS activation (Fig. 2B). Several controversial results exist in the literature on ACE2 expression and cigarette exposure (Brake et al. 2020; Ferrari et al. 2007, 2008; Oakes et al. 2018; Smith et al. 2020; Yilin et al. 2015). Previous studies have reported that nicotine has the potential to downregulate ACE2 expression in certain tissues or cell types (Ferrari et al. 2007, 2008; Oakes et al. 2018). However, CSE has a higher impact on ACE2 reduction in Calu-3 cells than in HTPE cells, which may not account for
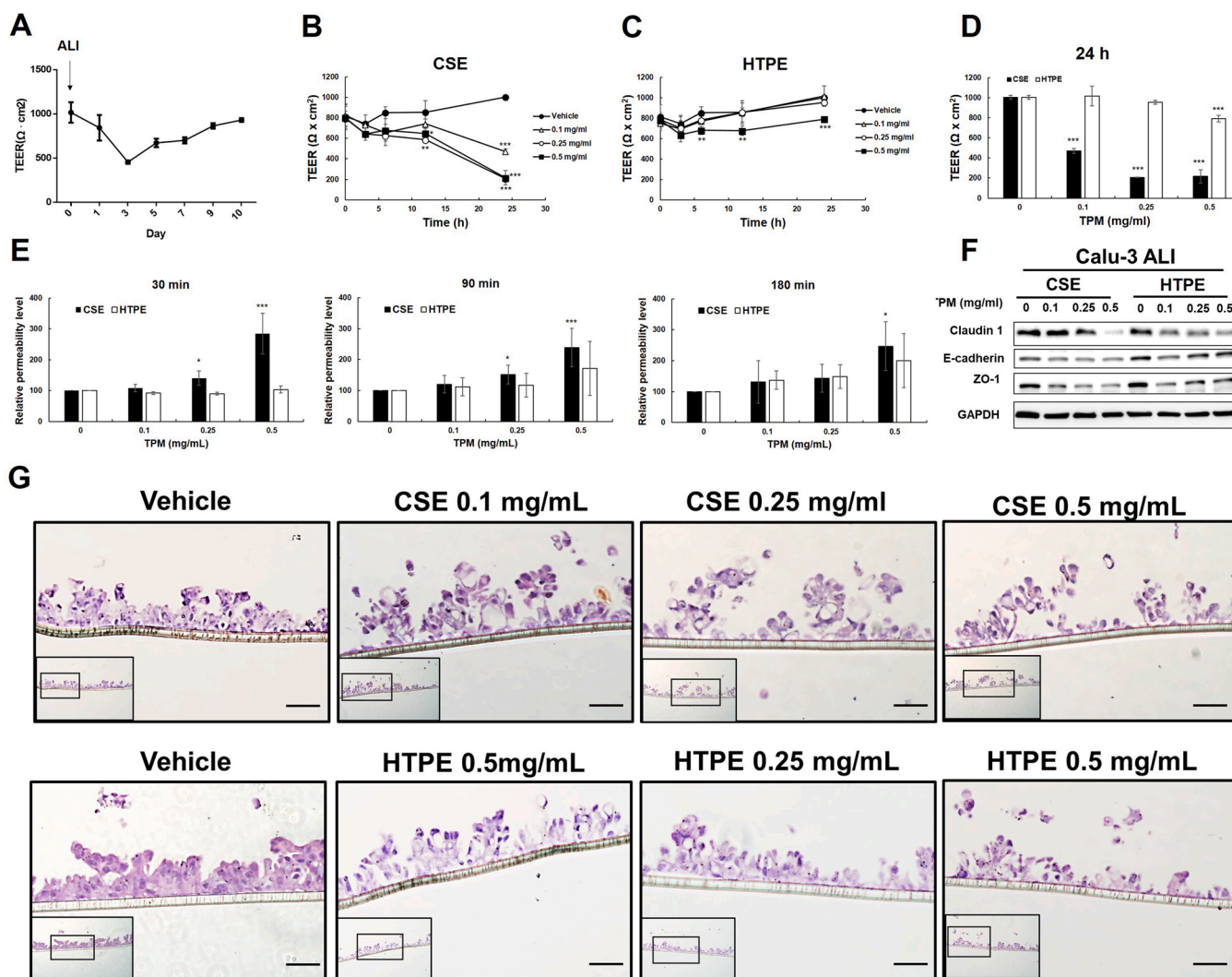
Fig. 4. The effect of CSE and HTPE on the epithelial barrier function of Calu-3 cultured in air-liquid interface (ALI). (A) The establishment of the ALI lung epithelial cell model consists of two stages: submerged culture (2–3 days) and ALI culture (10 days). Measurement of transepithelial electrical resistance (TEER) on day 1 to day 10 of ALI culture. (B-C) On day 10 of ALI culture, Calu-3 was treated with CSE (0–0.5 mg/mL, B) or HTPE (0–0.5 mg/mL, C) for 3–24 h, followed by measurement of TEER. (D-E) After 24 h-treatment of CSE or HTPE for 24 h, Calu-3 was analyzed by measurement of (D) TEER and (E) permeability assay using fluorescein iso-thiocyanate (FITC)-conjugated dextran (4 kDa, Sigma) at 30, 90 or 120 min. Values are presented as mean ± SD. Student's *t*-tests were used to determine statistical significance, and two-tailed p-values were shown. *p < 0.05, **p < 0.01, ***p < 0.005 compared with control group. (F) Western blot analysis of tight junction proteins including claudin-1, E-cadherin, and ZO-1 in Calu-3 cells cultured in ALI and treated with CSE (0–0.5 mg/mL) or HTPE (0–0.5 mg/mL) for 24 h. (G) Tissue morphology following exposure to CSE or HTPE in Calu-3 cultured in ALI. After 24 h treatment of CSE or HTPE in Calu-3 in ALI, tissues were fixed, paraffin-embedded, sectioned and stained by H&E to visualize tissue morphology. Representative images of control treatments, CSE-exposed cells, and HTPE-exposed cells were shown. Scale bar, 50 μm. A minimum of three independent experiments were performed.

nicotine levels since higher nicotine levels were detected in HTPE cells than in CSE cells in this study (Supplementary Fig. 2). Different substances in cigarettes, including nicotine and carbonyl compounds, may affect ACE2 differently than whole smoke, and smoking itself could alter ACE2 levels. Thus, the underlying mechanisms by which CSE or HTPE reduces ACE2 protein need further investigation.

Disruption of lung barrier integrity is increasingly linked to airway diseases (Aghapour et al. 2018; Rezaee and Georas, 2014). Our experiments on the bronchial epithelium revealed that CSE and HTPE exposure caused downregulation of tight junction proteins and disruption of TJ and AJ proteins in Calu-3 and Beas-2B cells (Fig. 3). Furthermore, the effects of CSE or HTPE on epithelial barrier function were evaluated using ALI cultures. The in vitro ALI model allows investigators to study particle interactions with the cells in an environment that more closely resembles the in vivo environment of the lung (He et al. 2021). Previous studies have shown that the Calu-3 epithelial model can retain its

monolayer structure and develop robust and tight junctions under long-term ALI culture; however, Beas-2B cells do not differentiate or form tight junctions (He et al. 2021). In this study, our results showed that CSE or a high dose of HTPE disrupted lung epidermal tight junctions using Calu-3 in ALI (Fig. 4). Furthermore, CSE or HTPE activated NF-kB pathways and increased the secretion of IL-6, IL-1β, and TNF-α (Supplementary Fig. 6). Together, these results indicate that both CSE and HTPE induced the release of inflammatory cytokines and disrupted tight junctions in Calu-3 cells in ALI.

There are several limitations to this study. First, we observed only an acute response to HTPE in an in vitro system. Second, we did not use whole aerosol/smoke, which smokers inhale. Third, we only used the SARS-CoV-2 spike protein S1 to mimic the binding process of SARS-CoV-2 infection. Thus, long-term, repeated whole aerosol/smoke exposure experiments and in vivo studies with animals and HTP users must be conducted to verify our in vitro cell-based results. Nevertheless, our
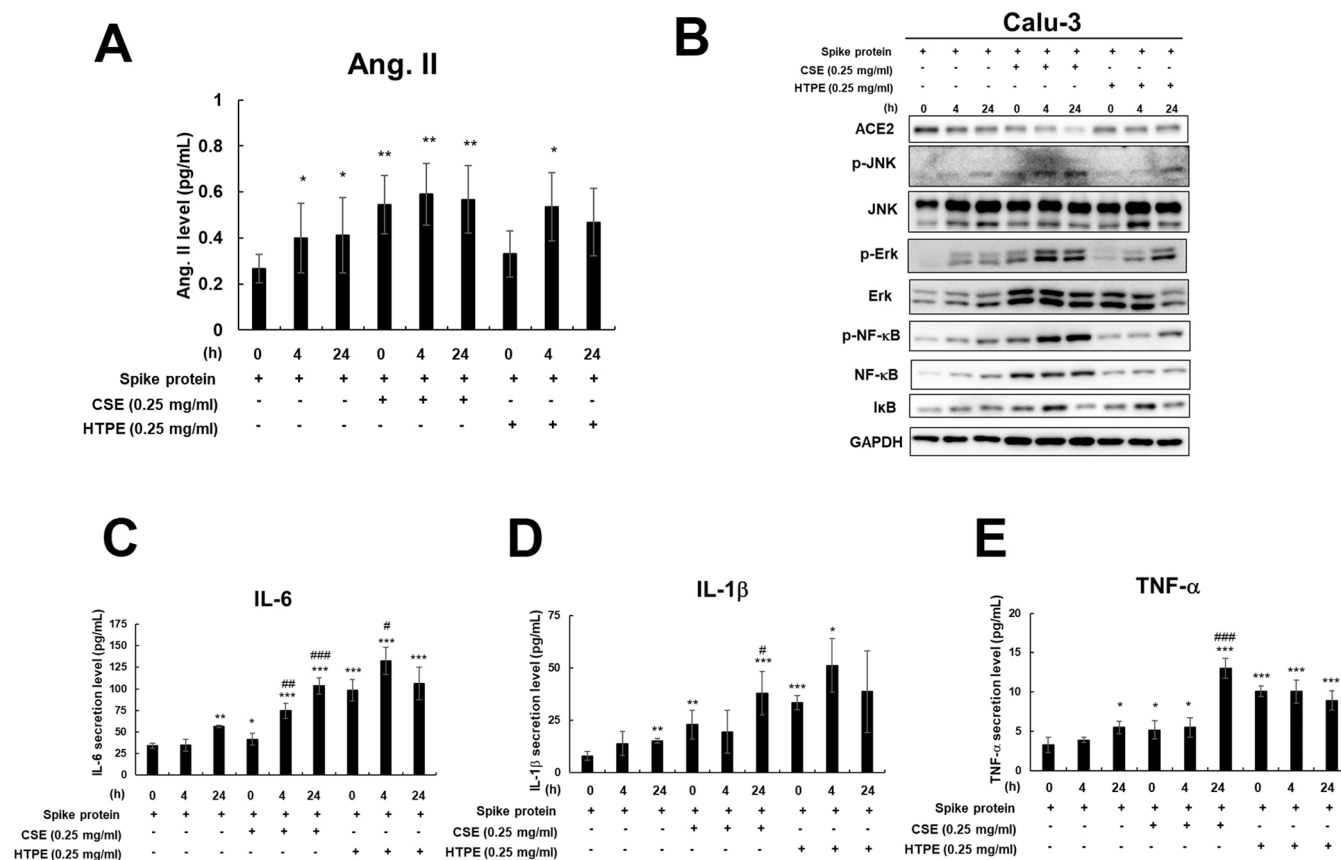
Fig. 5. The effect of CSE and HTPE on SARS-CoV-2 spike protein S1-induced lung injury responses. To mimic SARS-CoV-2 infection and study SARS-CoV-2 induced cellular injury, we stimulated Calu-3 cells with SARS-CoV2 spike protein S1 (aa 14–683) (Invitrogen # RP-87681, 10 ng/mL) for 0, 4, and 24 h after treatment of CSE or HTPE for 24 h. Since spike protein S1 was fused to His-Avi Tag at C-terminus, cells were stimulated with the peptide encoding the His-Avi Tag (His-Avi as a negative control). (A) The secretion of angiotensin II (Ang. II) was analyzed using the Angiotensin II ELISA kit (Sigma). (B) Western blot analysis of ACE2 and downstream MAPK pathway including p-JNK, p-ERK, and NF-kB inflammatory pathways including p-NF-kB, NF-kB, and Ik-B in Calu-3. (C-E) The secretion of IL-6, IL-1β, and TNFα in Calu-3 was analyzed using the IL-6, IL-1β, and TNFα ELISA kit (Invitrogen). Values are presented as mean ± SD. Student's t-tests were used to determine statistical significance, and two-tailed p-values were shown. *$p < 0.05$, **$p < 0.01$, ***$p < 0.005$ compared with cells without spike protein. #$p < 0.05$, ##$p < 0.01$, ###$p < 0.005$ compared with cells treated with CSE or HTPE in the absence of spike protein. A minimum of three independent experiments were performed.

acute exposure model shows that HTPs have the potential to cause lung injury, which is consistent with several previous studies (Davis et al. 2019; Glantz 2018b; Leigh et al. 2018; Moazed et al. 2018; Nabavizadeh et al. 2018; Sohal et al. 2019). Furthermore, two case reports showed that HTPs cause acute eosinophilic pneumonia, and these results strongly support that HTPs induce damage to the lungs (Aokage et al. 2019; Kamada et al. 2016).

5. Conclusions

Given our current findings and those of previous studies, HTPE can alter the RAS and increase inflammation and airway remodeling in airways, similar to CSE, leading to the pathogenesis of COPD. Intriguingly, HTPE, similar to CSE, has the potential to enhance the SARS-CoV-2-induced lung injury response. This study provides an efficient respiratory system to analyze the inhalation toxicity of newly developed cigarette products, and the results will help in the risk assessment and regulation of these products.

CRediT authorship contribution statement

H-H T, P-H W, T-Y L, and H-T W designed and performed research. H-H T, P-H W, T-H T, Y-H P, H-W C, and H-T W performed the experiments and analyzed the data. H-T W wrote the paper.

Declaration of Competing Interest

The authors declare that they have no known competing financial interests or personal relationships that could have appeared to influence the work reported in this paper.

Data availability

Data will be made available on request.

Appendix A. Supporting information

Supplementary data associated with this article can be found in the online version at doi:10.1016/j.tox.2022.153318.

References

Aghapour, M., Raee, P., Moghaddam, S.J., Hiemstra, P.S., Heijink, I.H., 2018. Airway epithelial barrier dysfunction in chronic obstructive pulmonary disease: role of cigarette smoke exposure. Am. J. Respir. Cell Mol. Biol. 58, 157–169.

Aokage, T., Tsukahara, K., Fukuda, Y., Tokioka, F., Taniguchi, A., Naito, H., Nakao, A., 2019. Heat-not-burn cigarettes induce fulminant acute eosinophilic pneumonia requiring extracorporeal membrane oxygenation. Respir. Med. Case Rep. 26, 87–90.

Barnes, P.J., Burney, P.G., Silverman, E.K., Celli, B.R., Vestbo, J., Wedzicha, J.A., Wouters, E.F., 2015. Chronic obstructive pulmonary disease. Nat. Rev. Dis. Prim. 1, 15076.

Benigni, A., Cassis, P., Remuzzi, G., 2010. Angiotensin II revisited: new roles in inflammation, immunology and aging. EMBO Mol. Med. 2, 247–257.

Biondi-Zoccai, G., Sciarretta, S., Bullen, C., Nocella, C., Violi, F., Loffredo, L., Pignatelli, P., Perri, L., Peruzzi, M., Marullo, A.G.M., De Falco, E., Chimenti, I., Cammisotto, V., Valenti, V., Coluzzi, F., Cavarretta, E., Carrizzo, A., Prati, F., Carnevale, R., Frati, G., 2019. Acute effects of heat-not-burn, electronic vaping, and traditional tobacco combustion cigarettes: the Sapienza University of Rome-Vascular Assessment of Proatherosclerotic Effects of Smoking (SUR - VAPES) 2 Randomized Trial. J. Am. Heart Assoc. 8, e010455.

Brake, S.J., Barnsley, K., Lu, W., McAlinden, K.D., Eapen, M.S., Sohal, S.S., 2020. Smoking upregulates angiotensin-converting enzyme-2 receptor: a potential adhesion site for novel coronavirus SARS-CoV-2 (Covid-19). J. Clin. Med. 9.

Chen, N., Zhou, M., Dong, X., Qu, J., Gong, F., Han, Y., Qiu, Y., Wang, J., Liu, Y., Wei, Y., Xia, J., Yu, T., Zhang, X., Zhang, L., 2020. Epidemiological and clinical characteristics of 99 cases of 2019 novel coronavirus pneumonia in Wuhan, China: a descriptive study. Lancet 395, 507–513.

Davis, B., To, V., Talbot, P., 2019. Comparison of cytotoxicity of IQOS aerosols to smoke from Marlboro Red and 3R4F reference cigarettes. Toxicol. In Vitro 61, 104652.

Dinakar, C., O'Connor, G.T., 2016. The health effects of electronic cigarettes. N. Engl. J. Med. 375, 1372–1381.

Donoghue, M., Hsieh, F., Baronas, E., Godbout, K., Gosselin, M., Stagliano, N., Donovan, M., Woolf, B., Robison, K., Jeyaseelan, R., Breitbart, R.E., Acton, S., 2000. A novel angiotensin-converting enzyme-related carboxypeptidase (ACE2) converts angiotensin I to angiotensin 1-9. Circ. Res. 87, E1–E9.

Dusautoir, R., Zarcone, G., Verriele, M., Garcon, G., Fronval, I., Beauval, N., Allorge, D., Riffault, V., Locoge, N., Lo-Guidice, J.M., Antherieu, S., 2021. Comparison of the chemical composition of aerosols from heated tobacco products, electronic cigarettes and tobacco cigarettes and their toxic impacts on the human bronchial epithelial BEAS-2B cells. J. Hazard. Mater. 401, 123417.

Edwards, M.R., Bartlett, N.W., Clarke, D., Birrell, M., Belvisi, M., Johnston, S.L., 2009. Targeting the NF-kappaB pathway in asthma and chronic obstructive pulmonary disease. Pharmacol. Ther. 121, 1–13.

Esposito, S., Galeone, C., Lelii, M., Longhi, B., Ascolese, B., Senatore, L., Prada, E., Montinaro, V., Malerba, S., Patria, M.F., Principi, N., 2014. Impact of air pollution on respiratory diseases in children with recurrent wheezing or asthma. BMC Pulm. Med. 14, 130.

Ferrari, M.F., Raizada, M.K., Fior-Chadi, D.R., 2007. Nicotine modulates the renin-angiotensin system of cultured neurons and glial cells from cardiovascular brain areas of Wistar Kyoto and spontaneously hypertensive rats. J. Mol. Neurosci. 33, 284–293.

Ferrari, M.F., Raizada, M.K., Fior-Chadi, D.R., 2008. Differential regulation of the renin-angiotensin system by nicotine in WKY and SHR glia. J. Mol. Neurosci. 35, 151–160.

Glantz, S.A., 2018a. Heated tobacco products: the example of IQOS. Tob. Control 27, s1–s6.

Glantz, S.A., 2018b. PMI's own in vivo clinical data on biomarkers of potential harm in Americans show that IQOS is not detectably different from conventional cigarettes. Tob. Control 27, s9–s12.

Guan, W.J., Ni, Z.Y., Hu, Y., Liang, W.H., Ou, C.Q., He, J.X., Liu, L., Shan, H., Lei, C.L., Hui, D.S.C., Du, B., Li, L.J., Zeng, G., Yuen, K.Y., Chen, R.C., Tang, C.L., Wang, T., Chen, P.Y., Xiang, J., Li, S.Y., Wang, J.L., Liang, Z.J., Peng, Y.X., Wei, L., Liu, Y., Hu, Y.H., Peng, P., Wang, J.M., Liu, J.Y., Chen, Z., Li, G., Zheng, Z.J., Qiu, S.Q., Luo, J., Ye, C.J., Zhu, S.Y., Zhong, N.S., 2020a. Clinical characteristics of coronavirus disease 2019 in China. N. Engl. J. Med. 382, 1708–1720.

Guan, W.J., Ni, Z.Y., Hu, Y., Liang, W.H., Ou, C.Q., He, J.X., Liu, L., Shan, H., Lei, C.L., Hui, D.S.C., Du, B., Li, L.J., Zeng, G., Yuen, K.Y., Chen, R.C., Tang, C.L., Wang, T., Chen, P.Y., Xiang, J., Li, S.Y., Wang, J.L., Liang, Z.J., Peng, Y.X., Wei, L., Liu, Y., Hu, Y.H., Peng, P., Wang, J.M., Liu, J.Y., Chen, Z., Li, G., Zheng, Z.J., Qiu, S.Q., Luo, J., Ye, C.J., Zhu, S.Y., Zhong, N.S., China Medical Treatment Expert Group for, C., 2020b. Clinical characteristics of coronavirus disease 2019 in China. N. Engl. J. Med. 382, 1708–1720.

He, R.W., Braakhuis, H.M., Vandebriel, R.J., Staal, Y.C.M., Gremmer, E.R., Fokkens, P.H.B., Kemp, C., Vermeulen, J., Westerink, R.H.S., Cassee, F.R., 2021. Optimization of an air-liquid interface in vitro cell co-culture model to estimate the hazard of aerosol exposures. J. Aerosol Sci. 153, 105703.

Heijink, I.H., Brandenburg, S.M., Postma, D.S., van Oosterhout, A.J., 2012. Cigarette smoke impairs airway epithelial barrier function and cell-cell contact recovery. Eur. Respir. J. 39, 419–428.

Heijink, I.H., Noordhoek, J.A., Timens, W., van Oosterhout, A.J., Postma, D.S., 2014. Abnormalities in airway epithelial junction formation in chronic obstructive pulmonary disease. Am. J. Respir. Crit. Care Med. 189, 1439–1442.

Hoek, G., Krishnan, R.M., Beelen, R., Peters, A., Ostro, B., Brunekreef, B., Kaufman, J.D., 2013. Long-term air pollution exposure and cardio- respiratory mortality: a review. Environ. Health Glob. Access Sci. Source 12, 43.

Ito, Y., Oshinden, K., Kutsuzawa, N., Kohno, C., Isaki, S., Yokoyama, K., Sato, T., Tanaka, M., Asano, K., 2020. Heat-Not-Burn cigarette induces oxidative stress response in primary rat alveolar epithelial cells. PLoS One 15, e0242789.

Jerng, J.S., Yu, C.J., Wang, H.C., Chen, K.Y., Cheng, S.L., Yang, P.C., 2006. Polymorphism of the angiotensin-converting enzyme gene affects the outcome of acute respiratory distress syndrome. Crit. Care Med. 34, 1001–1006.

Kamada, T., Yamashita, Y., Tomioka, H., 2016. Acute eosinophilic pneumonia following heat-not-burn cigarette smoking. Respirol. Case Rep. 4, e00190.

Kaparianos, A., Argyropoulou, E., 2011. Local renin-angiotensin II systems, angiotensin-converting enzyme and its homologue ACE2: their potential role in the pathogenesis of chronic obstructive pulmonary diseases, pulmonary hypertension and acute respiratory distress syndrome. Curr. Med. Chem. 18, 3506–3515.

Kuba, K., Imai, Y., Penninger, J.M., 2006. Angiotensin-converting enzyme 2 in lung diseases. Curr. Opin. Pharmacol. 6, 271–276.

Lee, W.L., Downey, G.P., 2001. Neutrophil activation and acute lung injury. Curr. Opin. Crit. Care 7, 1–7.

Leigh, N.J., Tran, P.L., O'Connor, R.J., Goniewicz, M.L., 2018. Cytotoxic effects of heated tobacco products (HTP) on human bronchial epithelial cells. Tob. Control 27, s26–s29.

Letko, M., Marzi, A., Munster, V., 2020. Functional assessment of cell entry and receptor usage for SARS-CoV-2 and other lineage B betacoronaviruses. Nat. Microbiol. 5, 562–569.

Liu, W., Tao, Z.W., Wang, L., Yuan, M.L., Liu, K., Zhou, L., Wei, S., Deng, Y., Liu, J., Liu, H.G., Yang, M., Hu, Y., 2020. Analysis of factors associated with disease outcomes in hospitalized patients with 2019 novel coronavirus disease. Chin. Med. J. 133, 1032–1038.

Lujan, H., Criscitiello, M.F., Hering, A.S., Sayes, C.M., 2019. Refining in vitro toxicity models: comparing baseline characteristics of lung cell types. Toxicol. Sci. 168, 302–314.

Lyu, Q., Jiang, L., Zheng, H., Hayashi, S., Sato, K., Toyokuni, S., 2022. Diluted aqueous extract of heat-not-burn tobacco product smoke causes less oxidative damage in fibroblasts than conventional cigarette. J. Clin. Biochem. Nutr. 71, 55–63.

Marshall, R.P., 2003. The pulmonary renin-angiotensin system. Curr. Pharm. Des. 9, 715–722.

Marshall, R.P., Webb, S., Bellingan, G.J., Montgomery, H.E., Chaudhari, B., McAnulty, R.J., Humphries, S.E., Hill, M.R., Laurent, G.J., 2002. Angiotensin converting enzyme insertion/deletion polymorphism is associated with susceptibility and outcome in acute respiratory distress syndrome. Am. J. Respir. Crit. Care Med. 166, 646–650.

Moazed, F., Chun, L., Matthay, M.A., Calfee, C.S., Gotts, J., 2018. Assessment of industry data on pulmonary and immunosuppressive effects of IQOS. Tob. Control 27, s20–s25.

Mosmann, T., 1983. Rapid colorimetric assay for cellular growth and survival: application to proliferation and cytotoxicity assays. J. Immunol. Methods 65, 55–63.

Munakata, S., Ishimori, K., Kitamura, N., Ishikawa, S., Takanami, Y., Ito, S., 2018. Oxidative stress responses in human bronchial epithelial cells exposed to cigarette smoke and vapor from tobacco- and nicotine-containing products. Regul. Toxicol. Pharmacol. 99, 122–128.

Nabavizadeh, P., Liu, J., Havel, C.M., Ibrahim, S., Derakhshandeh, R., Jacob Iii, P., Springer, M.L., 2018. Vascular endothelial function is impaired by aerosol from a single IQOS HeatStick to the same extent as by cigarette smoke. Tob. Control 27, s13–s19.

Nishida, K., Brune, K.A., Putcha, N., Mandke, P., O'Neal, W.K., Shade, D., Srivastava, V., Wang, M., Lam, H., An, S.S., Drummond, M.B., Hansel, N.N., Robinson, D.N., Sidhaye, V.K., 2017. Cigarette smoke disrupts monolayer integrity by altering epithelial cell-cell adhesion and cortical tension. Am. J. Physiol. Lung Cell Mol. Physiol. 313, L581–L591.

Oakes, J.M., Fuchs, R.M., Gardner, J.D., Lazartigues, E., Yue, X., 2018. Nicotine and the renin-angiotensin system. Am. J. Physiol. Regul. Integr. Comp. Physiol. 315, R895–R906.

Oldenburger, A., Poppinga, W.J., Kos, F., de Bruin, H.G., Rijks, W.F., Heijink, I.H., Timens, W., Meurs, H., Maarsingh, H., Schmidt, M., 2014. A-kinase anchoring proteins contribute to loss of E-cadherin and bronchial epithelial barrier by cigarette smoke. Am. J. Physiol. Cell Physiol. 306, C585–C597.

Paumgartten, F., 2018. Heat-not-burn and electronic cigarettes: truths and untruths about harm reduction. Rev. Assoc. Med. Bras. 64, 104–105.

Polosa, R., Caponnetto, P., 2016. The health effects of electronic cigarettes. N. Engl. J. Med. 375, 2608.

Rahman, I., Adcock, I.M., 2006. Oxidative stress and redox regulation of lung inflammation in COPD. Eur. Respir. J. 28, 219–242.

Raiden, S., Nahmod, K., Nahmod, V., Semeniuk, G., Pereira, Y., Alvarez, C., Giordano, M., Geffner, J.R., 2002. Nonpeptide antagonists of AT1 receptor for angiotensin II delay the onset of acute respiratory distress syndrome. J. Pharmacol. Exp. Ther. 303, 45–51.

Rezaee, F., Georas, S.N., 2014. Breaking barriers. New insights into airway epithelial barrier function in health and disease. Am. J. Respir. Cell Mol. Biol. 50, 857–869.

Schamberger, A.C., Mise, N., Jia, J., Genoyer, E., Yildirim, A.O., Meiners, S., Eickelberg, O., 2014. Cigarette smoke-induced disruption of bronchial epithelial tight junctions is prevented by transforming growth factor-beta. Am. J. Respir. Cell Mol. Biol. 50, 1040–1052.

Scharf, P., da Rocha, G.H.O., Sandri, S., Heluany, C.S., Pedreira Filho, W.R., Farsky, S.H. P., 2021. Immunotoxic mechanisms of cigarette smoke and heat-not-burn tobacco vapor on Jurkat T cell functions. Environ. Pollut. 268, 115863.

Schuliga, M., 2015. NF-kappaB signaling in chronic inflammatory airway disease. Biomolecules 5, 1266–1283.

Shrikrishna, D., Astin, R., Kemp, P.R., Hopkinson, N.S., 2012. Renin-angiotensin system blockade: a novel therapeutic approach in chronic obstructive pulmonary disease. Clin. Sci. 123, 487–498.

Simonavicius, E., McNeill, A., Shahab, L., Brose, L.S., 2018. Heat-not-burn tobacco products: a systematic literature review. Tob. Control.

Smith, J.C., Sausville, E.L., Girish, V., Yuan, M.L., Vasudevan, A., John, K.M., Sheltzer, J. M., 2020. Cigarette smoke exposure and inflammatory signaling increase the expression of the SARS-CoV-2 receptor ACE2 in the respiratory tract. Dev. Cell 53, 514–529 e513.

Sohal, S.S., Eapen, M.S., Naidu, V.G.M., Sharma, P., 2019. IQOS exposure impairs human airway cell homeostasis: direct comparison with traditional cigarette and e-cigarette. ERJ Open Res. 5.

Soleimani, F., Dobaradaran, S., De-la-Torre, G.E., Schmidt, T.C., Saeedi, R., 2022. Content of toxic components of cigarette, cigarette smoke vs cigarette butts: a comprehensive systematic review. Sci. Total Environ. 813, 152667.

Stewart, C.E., Torr, E.E., Mohd Jamili, N.H., Bosquillon, C., Sayers, I., 2012. Evaluation of differentiated human bronchial epithelial cell culture systems for asthma research. J. Allergy 2012, 943982.

Tabuchi, T., Kiyohara, K., Hoshino, T., Bekki, K., Inaba, Y., Kunugita, N., 2016. Awareness and use of electronic cigarettes and heat-not-burn tobacco products in Japan. Addiction 111, 706–713.

Tipnis, S.R., Hooper, N.M., Hyde, R., Karran, E., Christie, G., Turner, A.J., 2000. A human homolog of angiotensin-converting enzyme. Cloning and functional expression as a captopril-insensitive carboxypeptidase. J. Biol. Chem. 275, 33238–33243.

Tsukita, S., Tanaka, H., Tamura, A., 2019. The claudins: from tight junctions to biological systems. Trends Biochem. Sci. 44, 141–152.

Vardavas, C.I., Nikitara, K., 2020. COVID-19 and smoking: a systematic review of the evidence. Tob. Induc. Dis. 18, 20.

Wang, H.T., Chen, T.Y., Weng, C.W., Yang, C.H., Tang, M.S., 2016. Acrolein preferentially damages nucleolus eliciting ribosomal stress and apoptosis in human cancer cells. Oncotarget.

Wang, H.T., Hu, Y., Tong, D., Huang, J., Gu, L., Wu, X.R., Chung, F.L., Li, G.M., Tang, M. S., 2012. Effect of carcinogenic acrolein on DNA repair and mutagenic susceptibility. J. Biol. Chem. 287, 12379–12386.

Yilin, Z., Yandong, N., Faguang, J., 2015. Role of angiotensin-converting enzyme (ACE) and ACE2 in a rat model of smoke inhalation induced acute respiratory distress syndrome. Burns 41, 1468–1477.

Zhang, H., Penninger, J.M., Li, Y., Zhong, N., Slutsky, A.S., 2020a. Angiotensin-converting enzyme 2 (ACE2) as a SARS-CoV-2 receptor: molecular mechanisms and potential therapeutic target. Intensive Care Med. 46, 586–590.

Zhang, J.J., Dong, X., Cao, Y.Y., Yuan, Y.D., Yang, Y.B., Yan, Y.Q., Akdis, C.A., Gao, Y.D., 2020b. Clinical characteristics of 140 patients infected with SARS-CoV-2 in Wuhan, China. Allergy.